L. Leyva, D. Castanheira, A. Silva and A. Gameiro, "Two-stage estimation algorithm based on interleaved OFDM for a cooperative bistatic ISAC scenario," 2022 IEEE 95th Vehicular Technology Conference: (VTC2022-Spring), 2022, pp. 1-6, doi: 10.1109/VTC2022-Spring54318.2022.9860521.

Two-stage estimation algorithm based on interleaved OFDM for a cooperative bistatic ISAC scenario

Leonardo Leyva
Instituto de Telecomunicações and University of Aveiro
Aveiro, Portugal
leoleval@av.it.pt

Daniel Castanheira
Instituto de Telecomunicações
Aveiro, Portugal
dcastanheira@av.it.pt

Adão Silva
Instituto de Telecomunicações and University of Aveiro
Aveiro, Portugal
asilva@av.it.pt

Atílio Gameiro
Instituto de Telecomunicações and University of Aveiro
Aveiro, Portugal
amg@ua.pt

***Abstract*—This paper considers a cooperative bistatic scenario for integrated sensing and communication (ISAC) paradigm, where transmitter and receiver base stations (BS) are connected through the front-haul to a central unit (CU), enabling cooperation. A multiple-input multiple-output (MIMO) configuration is considered in combination with orthogonal frequency division multiplexing (OFDM). The communication and radio-sensing functions are performed in orthogonal sets of sub-carriers, where the sub-carriers allocated to radio-sensing are distributed among antennas in an interleaved way. The interleaved frame structure is exploited in the design of a new parameter estimation method. The proposed method is a two-stage algorithm to estimate the delay/Doppler shift and angular position of objects (paths) in the channel. First, the multiple signal classification (MUSIC) algorithm estimates the angle-of-arrival (AoA) of the paths. Then, the delay, Doppler shift and angle-of-departure (AoD) are jointly estimated for each AoA combining an extended search over the AoD domain and a two-dimensional periodogram. The simulations show that the delay, Doppler shift and AoA are estimated correctly, while the estimation of the AoD may report error, although it can be compensated.**

***Index Terms*—OFDM, MIMO, radar, MUSIC, periodogram, AoA/AoD estimation**

I. Introduction

The Orthogonal Frequency Division Multiplexing (OFDM) waveform is widely used by wireless communication systems, such as Long Term Evolution (LTE) and recently 5G New Radio (NR). Its ability to cope with severe channel conditions, high spectral efficiency and ease of implementation make it to be adopted for wireless communications, but it can be also used for radar and integrated sensing and communication (ISAC) paradigm [1] [2]. A pioneer work implementing OFDM for radio-estimation is presented in [3], which requires high computational effort due to the correlations between the frequency-shifted replicas and the transmitted signal. Other approaches based on correlation were further proposed, but they reported similar drawbacks, namely high computational complexity and range/Doppler ambiguities due to cyclic prefix (CP) and data dependency [1].

The work in [4] addresses several of the issues raised by the correlation approaches. A simple processing algorithm for OFDM radar was proposed, where the CP is first removed and the data-dependency is eliminated by a simple element-wise division between the baseband received signal and the transmitted symbols. Further contributions to [4] extended the algorithm to estimate the Doppler shift. They also cope with a multi-path and multi-user scenarios. These contributions are comprehensively reviewed in [1] [2]. Besides the simplicity, these methods provide the possibility of simultaneously conveying communication data and performing radio-sensing, but they are limited to range/Doppler estimation.

Multiple antennas enable the estimation of the angular direction of radio signals. The work in [5] extended the contribution in [1], to incorporate the estimation of the angle-of-arrival (AoA). Here, it is adopted a spectrally interleaved OFDM approach that preserves the range resolution while holding the orthogonality between the transmitted signals [6]. The authors in [7] compared the estimation performance of several interleaved OFDM multiple-input multiple-output (MIMO) schemes. The work in [8] studied the performance of OFDM-based commercial communication waveforms for radio-sensing applications, with a focus on LTE and 5G NR. More recently, the authors of [9] proposed an algorithm that exploits the empty sub-carries within an OFDM frame using optimized samples to enhance the radio-sensing performance. These contributions, exploiting the structure of the OFDM frame for radar applications, are limited to the monostatic topology.

The exploitation of the OFDM frame for a bi-static radar topology has been considered in [10]. Here, the authors validated the OFDM-based signal processing, described in [1], for a practical bi-static setup considering a moving vehicle. Furthermore, the work in [11] validated the OFDM waveform in a distributed bi-static radar topology. The results showed that it is possible to detect and estimate targets parameters (e.g., delay and Doppler shift) of moving cars and even pedestrians. Similar to [8], [12] evaluates LTE for radar processing, but now considering a bi-static setup and studies the ambiguity function (AF) of the delay and Doppler shift obtained for the synchronization and reference signals of the downlink LTE link.

This paper is based on the general scenario in [13], where the base stations (BS) are connected through the front-haul

This work has received funding from the European Union's Horizon 2020 research and innovation programme under the Marie Skłodowska-Curie ETN TeamUp5G, grant agreement No. 813391.

to a central unit (CU) for joint processing. Concerning the communication component, the BSs deal with the users equipment (UE) in one cell and may benefit from cooperation, while for the sensing component, sets of BSs are organized in complementary Tx/Rx pairs, allowing cooperative sensing of the environment, relying on the fixed network elements. In this paper, we focus on the sensing component of a Tx/Rx pair, where the Tx ISAC BS multiplexes communication and radar functionalities in frequency, i.e., different sets of subcarriers are used for sensing and communication, respectively. Besides, the proposed radio-sensing algorithm relies on spectrally interleaved OFDM waveform [5]. The goal is to estimate the parameters of the objects (paths) that made up the channel, i.e., delay, Doppler, AoA and angle-of-departure (AoD). This work presents a two-stage radio-sensing estimation algorithm for a bi-static ISAC paradigm. The main contributions are the cooperative component, and the exploitation of the spectrally interleaved OFDM frame to estimate the AoD. The cooperative component enabled by the CU allows the receiver to know the transmitted symbols, which is used by the radio-sensing estimation algorithm. On the other hand, the algorithm exploits the specific frequency/spatial allocation of subcarriers of spectrally interleaved OFDM to jointly estimates the AoD, delay and Doppler shift. Besides, it is demonstrated that the error in the estimate of the AoD can be compensated. The proposed algorithm is divided into two stages, the first phase relies on MUSIC to estimate the AoAs, while the second phase jointly estimates the remaining parameters through a combination of extended search over the domain of the AoD and two-dimensional periodogram. Simulation results confirm the effectiveness of the two-stage algorithm for the estimation of AoA, delay, and Doppler shift for several waveform parameterizations. However, as it will be discussed, the AoD estimate is biased. But, although the error can be severe, it can be compensated as it will be shown in this work.

The remainder of this paper is organized as follows: Section II introduces the system model. Section III describes the proposed two-stage OFDM-based estimation algorithm. Section IV assesses the proposed algorithm in terms of delay/Doppler, AoD and AoA estimation through several waveform parameterizations. Finally, section IV concludes this paper.

II. System Model

The scenario in Fig. 1 considers a cooperative bi-static topology, i.e. a single Tx/Rx pair. It represents a simplification of the more general scenario proposed in [13]. In this setup, the transmitter and receiver BSs are equipped with uniform linear arrays (ULAs) of N_{tx} and N_{rx} antennas, respectively. In this paper, the transmitter BS multiplexes the communication and sensing function in the frequency domain. Two sets of orthogonal sub-carriers are considered, one for the sensing and the other for the communication functionality. For the radio-sensing set of sub-carriers, there is considered spectrally interleaved OFDM, while for the communication set of sub-carriers, beamforming aspects may be considered. In this scenario, the N_c available sub-carriers may be conveniently divided into N_r and N_s blocks of sub-carriers for radar and communication, respectively. The allocation of the sub-carriers relies on the desired radar/communication performance metrics like data rate or range resolution. However, for ease of description, this work concentrates on the radar parameter estimation and assumes that the N_c sub-carriers are exploited by the radar function.

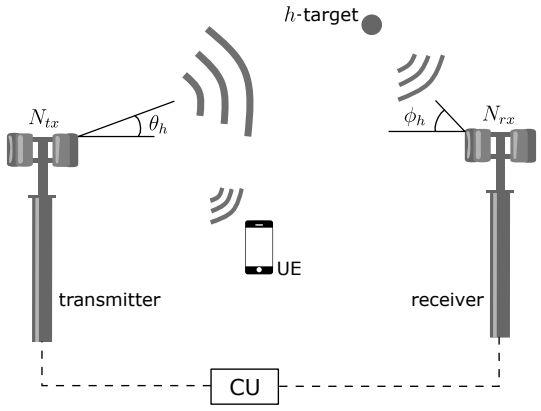

Fig. 1. Cooperative bistatic radar topology.

It is considered that the system operates in the millimetre-wave band (mmWave). Therefore, the received signal at the receiver BS [14] can be described by,

$$\mathbf{Y} = \sum_{h=1}^{H} \beta_h \mathbf{b}\left(\phi_h\right) \mathbf{a}^T\left(\theta_h\right) \tilde{\mathbf{X}}_h + \mathbf{N}, \tag{1}$$

where H is the number of scattering paths, β_h stands as the complex scattering coefficient, and $\mathbf{a}(\theta_h) \in \mathbb{C}^{N_{\text{tx}} \times 1}$ and $\mathbf{b}(\phi_h) \in \mathbb{C}^{N_{\text{rx}} \times 1}$ describes the transmitter and receiver steering vectors, respectively. For an ULA with N antennas, the steering vector is described by

$$\mathbf{a}(\theta) = \frac{1}{\sqrt{N}} \left[1,\ e^{-j\frac{2\pi}{\lambda} d \sin(\theta)},\ \cdots,\ e^{-j\frac{2\pi}{\lambda} d(N-1)\sin(\theta)}\right]^T, \tag{2}$$

where λ and d are the signal wavelength and the spacing between consecutive antenna elements. The matrix $\tilde{\mathbf{X}}_h$ describes the delayed and Doppler-shifted version of the transmitted signal $\mathbf{X} \in \mathbb{C}^{N_{\text{tx}} \times T}$ for the h-th path, and T is the number of samples [14]. Finally, $\mathbf{N} \in \mathbb{C}^{N_{\text{rx}} \times T}$ represents the additive white Gaussian noise (AWGN), which elements are *i.i.d.* complex Gaussian random variables with zero mean and variance σ_n^2.

From [6], it is known that the estimation of the parameters of objects is optimized when the N_{tx} transmitted waveforms are orthogonal, i.e., $\frac{1}{T}\mathbf{X}\mathbf{X}^H = \frac{P_T}{N_{\text{tx}}}\mathbf{I}_{N_{\text{tx}}}$. This requirement can be satisfied by interleaving the N_c sub-carriers along the N_{tx} transmitting antennas [5]. Therefore, the entry of $\mathbf{X}$ corresponding to the p antenna element and the n fast-time sample of an OFDM symbol is given by,

$$\mathbf{X}_{p,n} = \sum_{q=0}^{N_c/N_{\text{tx}}-1} c_{k_{p,q},l} \exp\left(j2\pi \frac{k_{p,q} n}{N_c}\right) \tag{3}$$

where $c_{k_{p,q},l}$ stands as the complex symbol transmitted by sub-carrier $k_{p,q}$ and the l OFDM symbol. The sub-carrier index $k_{p,q}$ follows the relation $k_{p,q} = p + qN_{\text{tx}}$, where p is the antenna element and q the sub-carrier index per antenna.

III. Radio-sensing estimation algorithm

This section presents the algorithm that estimates the parameters of the H objects, namely, AoA, delay, Doppler shift and AoD. The algorithm is divided into two phases: the first phase uses the multiple signal classification (MUSIC) algorithm to estimate the AoAs, and the second phase estimates the remaining parameters through a combination of extended search over the AoD domain and spectral estimation based on two-dimensional periodogram [1].

A. Estimation of the AoAs

For ease of explanation, the received signal in (1) can be rewritten in matrix notation as,

$$\mathbf{Y} = \mathbf{B}\mathbf{S}_{\mathbf{X}} + \mathbf{N}, \tag{4}$$

where $\mathbf{B} = [\mathbf{b}(\phi_1)\,\mathbf{b}(\phi_2)\cdots\mathbf{b}(\phi_H)] \in \mathbb{C}^{N_{\text{rx}}\times H}$ is the Vandermonde matrix of receiving steering vectors, and the matrix $\mathbf{S}_{\mathbf{X}}$ is described by,

$$\mathbf{S}_{\mathbf{X}} = \begin{bmatrix} \beta_1\mathbf{a}^T(\theta_1)\tilde{\mathbf{X}}_1 \\ \beta_2\mathbf{a}^T(\theta_2)\tilde{\mathbf{X}}_2 \\ \vdots \\ \beta_H\mathbf{a}^T(\theta_H)\tilde{\mathbf{X}}_H \end{bmatrix} \in \mathbb{C}^{H\times T} \tag{5}$$

where, the H scattered versions of the transmitted signal $\mathbf{X}$ incorporates the delay, Doppler shift and the phase shift due to the AoD for the h-th object that will be estimated in the second stage. The MUSIC algorithm computes the auto-correlation matrix of the received signal [14] as

$$\mathbf{R}_Y = \frac{1}{T}\mathbf{Y}\mathbf{Y}^H = \frac{1}{T}\mathbf{B}\mathbf{S}_{\mathbf{X}}\mathbf{S}_{\mathbf{X}}{}^H\mathbf{B}^H + \frac{1}{T}\mathbf{N}\mathbf{N}^H \tag{6}$$

$$\approx \mathbf{B}\mathbf{R}_{\mathbf{S}_{\mathbf{X}}}\mathbf{B}^H + \sigma_n^2\mathbf{I}_{N_{\text{rx}}}, \tag{7}$$

where, the singular value decomposition (SVD) of (7) can be represented by

$$\mathbf{R}_Y = \mathbf{U}\boldsymbol{\Delta}\mathbf{V}^H, \tag{8}$$

if the eigenvalues in (8) are sorted in decreasing order, the first H columns of $\mathbf{U} = [\mathbf{S} \quad \mathbf{G}]$ span the signal subspace $\mathbf{S} \in \mathbb{C}^{N_{\text{rx}}\times H}$, while the remaining $N_{\text{rx}} - H$ columns span the noise subspace $\mathbf{G} \in \mathbb{C}^{N_{\text{rx}}\times(N_{\text{rx}}-H)}$. Therefore, the MUSIC spectrum is obtained by,

$$\hat{P}_{\text{MU}}\left(\hat{\phi}\right) = \frac{1}{\mathbf{b}^H\left(\hat{\phi}\right)\mathbf{G}\mathbf{G}^H\mathbf{b}\left(\hat{\phi}\right)} \tag{9}$$

where, the H largest values correspond to the AoAs of the objects. Here, we assume that the objects are resolvable, i.e., the AoAs of the objects are spaced for more than the resolution of the receiver ULA. Therefore, the matrix that filters the H paths can be described by

$$\hat{\mathbf{B}} = [\mathbf{b}(\hat{\phi}_1)\,\mathbf{b}(\hat{\phi}_2)\cdots\mathbf{b}(\hat{\phi}_H)] \in \mathbb{C}^{N_{\text{rx}}\times H}, \tag{10}$$

which is the Vandermonde matrix formulated from the H estimated AoAs.

B. Estimation of delay, Doppler shift and AoD

This section describes the method that estimates the delay, Doppler shift and AoD at the bistatic receiver. First, the received signal is separated into the signals corresponding to the AoAs estimated in the previous section. Then, the individual signals are processed and the transmitted data, known through the cooperative scheme, is removed. This returns the channel response matrix for N_c subcarriers and M OFDM symbols, from which, the delay, Doppler shift and AoD are estimated. The algorithm exploits the interleaved structure of the OFDM frame to jointly estimate the parameters through a combination of extended search over the domain of the AoD and two-dimensional periodogram, by matching the received with the transmitted waveform.

The received signal in (4) is multiplied by the matrix in (10)

$$\hat{\mathbf{Y}} = \hat{\mathbf{B}}^H\mathbf{Y} \tag{11}$$

$$= \hat{\mathbf{B}}^H\mathbf{B}\mathbf{S}_{\mathbf{X}} + \hat{\mathbf{B}}^H\mathbf{N} \tag{12}$$

$$\simeq \mathbf{S}_{\mathbf{X}} + \hat{\mathbf{N}}, \tag{13}$$

where, if $N_{\text{rx}} \gg H$ and the H objects are resolvable, then $\mathbf{b}(\hat{\phi_h})^H\mathbf{b}(\phi_i) \approx 0$ for $i \neq h$, i.e., $\mathbf{B}^H\mathbf{B} \approx \mathbf{I}_H$. After CP removal and fast Fourier transform (FFT) of length N_c over each row in (13) through M OFDM symbols, we get H matrices like $\mathbf{F}_{\hat{\mathbf{Y}}_h} \in \mathbb{C}^{N_c\times M}$ for the h-th path. For $\mathbf{F}_{\hat{\mathbf{Y}}_h}$, the entry corresponding to the $k_{p,q}$ sub-carrier and l OFDM symbol [8] is given by

$$(\mathbf{F}_{\hat{\mathbf{Y}}_h})_{k_{p,q},l} = e^{-j\frac{2\pi}{\lambda}dp\sin(\theta_h)}f(\tau_h, f_{D,h})c_{k_{p,q},l} + (\tilde{\mathbf{N}})_{k_{p,q},l}, \tag{14}$$

where, $\tilde{\mathbf{N}}$ is the matrix representation of the AWGN, the term $e^{-j\frac{2\pi}{\lambda}dp\sin(\theta_h)}$ is the phase shift of the p antenna element of the transmitting steering vector

$$\mathbf{a}(\theta_h) = \frac{1}{\sqrt{N_{\text{tx}}}}\left[1,\ e^{-j\frac{2\pi}{\lambda}d\sin(\theta_h)}, \cdots, e^{-j\frac{2\pi}{\lambda}d(N_{\text{tx}}-1)\sin(\theta_h)}\right]^T, \tag{15}$$

θ_h represents the AoD of the h-th path, $c_{k_{p,q},l}$ is the data symbol, and $f(\tau_h, f_{D,h})$ is a function of the delay and Doppler shift described by,

$$f(\tau_h, f_{D,h}) = e^{j2\pi f_{D_h}lT_{sym}}e^{-j2\pi k_{p,q}\Delta f\tau_h} \tag{16}$$

where, the term $e^{j2\pi f_{D_h}lT_{sym}}$ modulates each row of $\mathbf{F}_{\hat{\mathbf{Y}}_h}$ with a Doppler shift f_{D_h} and T_{sym} is the OFDM symbol duration, while $e^{-j2\pi k_{p,q}\Delta f\tau_h}$ modulates each column of $\mathbf{F}_{\hat{\mathbf{Y}}_h}$ with a different phase shift for every sub-carrier $k_{p,q}$ depending of the delay τ_h.

The algorithm continues by eliminating the transmitted symbols $c_{k_{p,q},l}$ from (14) by an element wise-division [1] like

$$(\mathbf{F}_h)_{k_{p,q},l} = \frac{(\mathbf{F}_{\hat{\mathbf{Y}}_h})_{k_{p,q},l}}{c_{k_{p,q},l}}. \tag{17}$$

Since the N_c sub-carriers are interleaved between the N_{tx} transmitting antennas, the steering vector in (15) repeats

N_c/N_{tx} times over the columns of $\mathbf{F}_h$, which can be rewritten like

$$\mathbf{F}_h = \begin{bmatrix} \hat{\mathbf{F}}_h^{(0)} \\ \hat{\mathbf{F}}_h^{(1)} \\ \vdots \\ \hat{\mathbf{F}}_h^{(N_c/N_{\text{tx}}-1)} \end{bmatrix} \in \mathbb{C}^{N_c \times M}, \tag{18}$$

where $\hat{\mathbf{F}}_h^{(q)} \in \mathbb{C}^{N_{\text{tx}} \times M}$ stands as the q sub-matrix of $\mathbf{F}_h$, where row p is associated with antenna p and q is the sub-carrier index per antenna, as in (3).

The algorithm continues by performing an extended search over the domain of the AoD, i.e., all possible angles ranging from $\omega = [-\pi/2\ ,\ \pi/2]$. The extended search is performed under the assumption that the channel frequency response of the sub-matrices $\hat{\mathbf{F}}_h^{(q)}$ is almost flat, i.e., the spectrally-interleaved OFDM allocates consecutive sub-carriers to the transmitter antennas (refer to (3)). The search steering matrix is defined as

$$\mathbf{A}(w) = \begin{bmatrix} \mathbf{a}(\omega)^H & \mathbf{0} & \cdots & \mathbf{0} \\ \mathbf{0} & \mathbf{a}(\omega)^H & & \mathbf{0} \\ \vdots & & \ddots & \vdots \\ \mathbf{0} & \mathbf{0} & \cdots & \mathbf{a}(\omega)^H \end{bmatrix} \in \mathbb{C}^{N_c/N_{\text{tx}} \times N_c}. \tag{19}$$

Therefore, the extended search is performed by multiplying $\tilde{\mathbf{F}}_h^{(\omega)} = \mathbf{A}(w)\mathbf{F}_h$, for $\omega = [-\pi/2\ ,\ \pi/2]$,

$$\tilde{\mathbf{F}}_h^{(\omega)} = \begin{bmatrix} \mathbf{a}(\omega)^H \hat{\mathbf{F}}_h^{(0)} \\ \mathbf{a}(\omega)^H \hat{\mathbf{F}}_h^{(1)} \\ \vdots \\ \mathbf{a}(\omega)^H \hat{\mathbf{F}}_h^{(N_c/N_{\text{tx}}-1)} \end{bmatrix} \in \mathbb{C}^{N_c/N_{\text{tx}} \times M}, \tag{20}$$

from which, the delay and Doppler shift is jointly estimated through a complex two-dimensional periodogram, which is a well-understood tool to resolve sinusoids in a discrete signal [1]. Therefore, for $\tilde{\mathbf{F}}_h^{(\omega)}$, the resulting periodogram is obtained by

$$\mathbf{P}_h^{(w)} = \mathrm{C}_{\text{PER}}(\tilde{\mathbf{F}}_h^{(\omega)}) \tag{21}$$

where $\mathrm{C}_{\text{PER}}(\cdot)$ stands as the two-dimensional periodogram operator over a given matrix. The periodograms obtained from (21) are stored in a three-dimensional array, defined as $\mathbf{P}_h$. The delay, Doppler shift and AoD for the h-th object are jointly estimated by finding the peak of $\mathbf{P}_h$ like,

$$\hat{\tau}_h, \hat{f}_{D_h}, \hat{\theta}_h = \text{fPe}(\mathbf{P}_h), \tag{22}$$

where the operator $\text{fPe}(\cdot)$ identifies the peak of the multi-dimensional array $\mathbf{P}_h$. The proposed algorithm that jointly estimate the delay, Doppler shift, and AoD is summarized as follows.

The algorithm 1 repeats for the H objects, i.e for the H matrices $\mathbf{F}_{\hat{\mathbf{Y}}_h}$ obtained from filtering the received signal $\mathbf{Y}$, and after CP removal, FFT over the rows of (13) thought M OFDM symbols.

Algorithm 1: Extended search and two-dimensional peridogram-based algorithm for jointly estimating τ_h, f_{D_h} and θ_h.

Result: $\hat{\tau}_h$; $\hat{f}_{D_h}$; $\hat{\theta}_h$
Input: $\mathbf{F}_{\hat{\mathbf{Y}}_h}$;
1. Remove data dependency ;
2. Get matrix $\mathbf{F}_h$ as in (18)
for ω: $-\pi/2$ *to* $\pi/2$ **do**
  3. Compute $\tilde{\mathbf{F}}_h^{(\omega)}$
  4. Obtain the two-dimensional peridogram: $\mathbf{P}_h^{(w)} = \mathrm{C}_{\text{PER}}(\tilde{\mathbf{F}}_h^{(\omega)})$
  5. $\mathbf{P}_h \leftarrow \mathbf{P}_h^{(w)}$
end
6. $\hat{\tau}_h, \hat{f}_{D_h}, \hat{\theta}_h = \text{fPe}(\mathbf{P}_h)$

IV. Results

The proposed method is evaluated in a scenario with five objects ($H = 5$), which parameters are summarized in Table I and compared with the Matched Filter (MF) approach [14]. The system operates in the 24 GHz, and the signal-to-noise ratio (SNR) is set to 10 dB. Besides, it is considered that the transmitter and receiver ULAs are equipped with 8 and 16 elements, respectively, separated by a distance of $\lambda/2$. In the following, the acronym PM refers to the proposed method, i.e., to differentiate from the MF.

TABLE I
Parameters of objects.

Object	AoA	delay	Doppler shift	AoD
1	$-17°$	0 us	4 kHz	$-50°$
2	$25°$	0.3072 us	2 kHz	$15°$
3	$43°$	0.7172 us	-4 kHz	$55°$
4	$-7°$	0.1526 us	-1 kHz	$-20°$
5	$10°$	0.5124 us	-5 kHz	$40°$

Due to the coherent combination of the transmitting antennas in (20) and the discrete nature of $\mathbf{P}_h^{(w)}$ [1], the maximum unambiguous delay is given by

$$\tau_{unamb} = \frac{1}{N_{\text{tx}} \Delta f} \tag{23}$$

and the maximum unambiguous Doppler shift is

$$f_{d_{unamb}} = \frac{1}{2T_{symb}}. \tag{24}$$

The maximum unambiguous delay and Doppler shift are set to 1 us and 7 kHz, which allow resolving objects at a maximum range/velocity of 300 meters and 150 km/h. Finally, the algorithm is assessed through two spectrally interleaved OFDM waveforms, which evaluates the impact of (20) in the estimate of the delay, Doppler shift, AoA and AoD. Waveform 1 and 2 are designed to fulfill (23) and (24) and the parameters are outlined in Table II.

TABLE II
OFDM WAVEFORM PARAMETERS

Parameters	OFDM param. 1	OFDM param. 2
Number of sub-carriers	1024	4096
Sampling frequency	78.06 MHz	57.344 MHz
Overall OFDM duration	14.11 us	72.43 us
Sub-carrier separation	76.230 kHz	14 kHz
OFDM symbols in a frame	64	16

The main difference between the waveforms parameterizations is the sub-carrier separation, which influences the coupling between the range/Doppler and space (AoD) domains. The higher the sub-carrier separation the higher the error in the AoD estimate.

A. AoA, delay and Doppler estimation

Table III presents the real and estimated AoA, considering both waveforms in Table II obtained for the proposed method and the MF approach.

TABLE III
REAL AND ESTIMATED AOA FOR THE PM AND MF.

Object	Real	PM wav.1	PM wav.2	MF
1	$-17°$	$-17°$	$-17°$	$-17°$
2	$25°$	$25°$	$25°$	$25°$
3	$43°$	$43°$	$43°$	$43°$
4	$-7°$	$-7°$	$-7°$	$-7°$
5	$10°$	$10°$	$10°$	$10°$

From Table III, it can be noticed that the AoA is correctly estimated for the PM and MF, and for both waveforms in Table II. Fig. 2 presents the estimate of the delay and Doppler shift obtained for both waveforms in Table II, considering the PM and the MF approach.

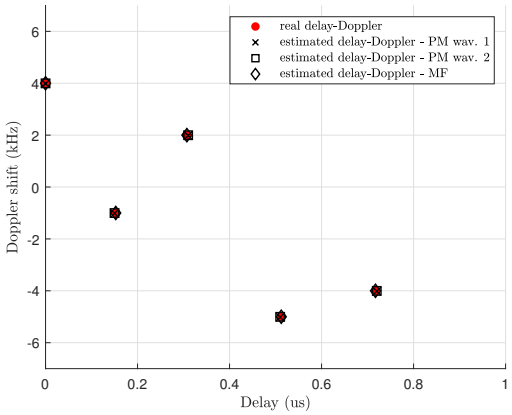

Fig. 2. Estimate of the delay and Doppler shift for objects in Table I, assessed for the PM (i.e., waveforms 1 and 2) and the MF approach.

Similar to the estimate of the AoA, Fig. 2 shows that the delay and Doppler shift are correctly estimated for the assessed waveforms and algorithms. It is worth noting that the resolution of the AoA, delay and Doppler shift can be enhanced by increasing the number of receiving antenna elements, bandwidth and number of OFDM symbols in the OFDM frame, respectively.

B. AoD estimation

The estimate of the AoDs for objects in Table I, evaluated for the proposed method, considering both waveforms 1 and 2 and the MF are presented in Table IV.

TABLE IV
REAL AND ESTIMATED AOD FOR THE PM AND MF.

Object	Real	PM wav.1	PM wav.2	MF
1	$-50°$	$-50°$	$-50°$	$-50°$
2	$15°$	$18°$	$15°$	$15°$
3	$55°$	$68°$	$57°$	$55°$
4	$-20°$	$-19°$	$-20°$	$-20°$
5	$40°$	$46°$	$41°$	$40°$

The results in Table IV show that the MF approach correctly estimates the AoD, while the proposed method reports errors. This is true for both of the evaluated waveforms, being more critical for waveform 1 (e.g., for $\theta_3 = 55°$, the resulting error for waveform 1 is $e_{\hat{\theta}_3} = 13°$, while for waveform 2 is $e_{\hat{\theta}_3} = 2°$). Although the MF presents better performance for the estimation of the AoD than the proposed method, the high computational effort makes it infeasible in practice.

The error reported by the proposed method is because the channel frequency response of the sub-matrices $\hat{\mathbf{F}}_h^{(q)}$ is not completely flat for path delay τ_h different from zero. Indeed, the channel frequency response is a function of Δf (i.e., waveform parameterization), τ_h and θ_h (refers to (14)). Therefore, $\mathbf{a}(\omega)^H \hat{\mathbf{F}}_h^{(q)}$ in (20) has a direct impact on the estimate of the AoD, which is characterized in the following section.

C. Error characterization of the AoD

The simulation in section IV-B shows that the proposed method reports errors in the estimate of the AoD. However, the observation of simulations varying the remaining parameters (i.e., delay, Doppler shift and AoA) and different waveform parameterizations revealed that the error is characterized as a function of the delay, AoD and waveform parameterization. Fig. 3 and 4 characterize the error for waveform 1 and 2, respectively.

From these results, it may be thought that waveform 2 (i.e., less sub-carrier separation) is more suitable than waveform 1, i.e., the maximum error reported for waveform 2 is $e_{\max} = 3°$ while for waveform 1 is $e_{\max} = 28°$. However, waveform 2 presents a drawback concerning the reduced maximum unambiguous Doppler shift (24), which is inversely proportional to the OFDM symbol duration. Besides, since the error can be characterized, waveform 1 can be also used and compensate for the error. For instance, Fig. 5 presents a "compensation curve" obtained for waveform 1 and delay ($\tau = 0.82$ us), the

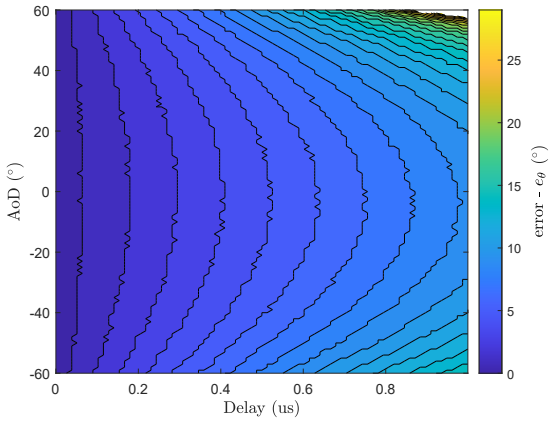

Fig. 3. Characterization of the error in the estimate of the AoD (assessed for waveform 1).

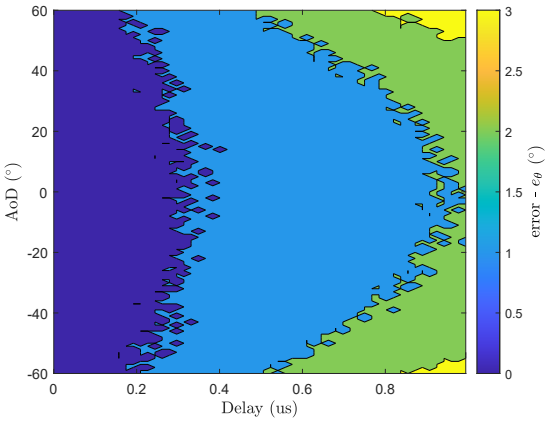

Fig. 4. Characterization of the error in the estimate of the AoD (assessed for waveform 2).

compensated AoD (y-axis in Fig. 5) is obtained by entering the curve with the estimated AoD (x-axis in Fig. 5).

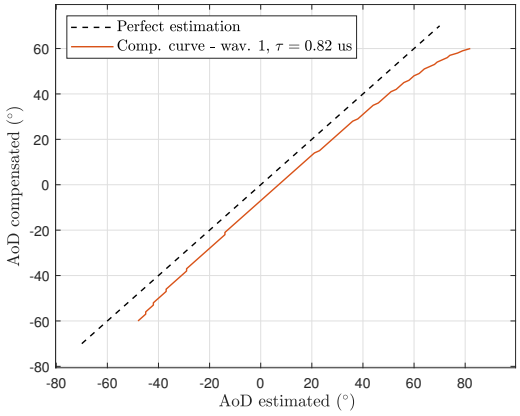

Fig. 5. Perfect estimation and compensation curve obtained for waveform 1 and $\tau = 0.82$ us.

V. Conclusions

In this paper, the estimation of the AoA, delay, Doppler shift and AoD of the objects that composite a sparse channel is achieved for a cooperative bistatic scenario, where the transmitter and receiver are connected through the front-haul to a central unit. The proposed algorithm exploits the spectrally interleaved OFDM frame and the cooperation to estimate the AoA, delay, Doppler shift and AoD. The algorithm first estimates the AoA by MUSIC algorithm and then the remaining parameters are jointly estimated through a combination of an extended search over the domain of the AoD and 2D-periodogram. The proposed method is assessed for a scenario with five objects and two different parameterizations of the spectrally interleaved OFDM waveform and compared to the MF. It is shown that the AoA, delay and Doppler shift are correctly estimated for the considered objects and waveforms. Furthermore, although the AoD estimation initially reports an error, it was shown that this can be compensated. These results are of interest to the radar community but also to the integrated sensing and communication community.

References

[1] C. Sturm and W. Wiesbeck, "Waveform Design and Signal Processing Aspects for Fusion of Wireless Communications and Radar Sensing," *Proc. IEEE*, vol. 99, no. 7, pp. 1236-1259, July 2011.

[2] B. Paul, A. R. Chiriyath and D. W. Bliss, "Survey of RF communications and sensing convergence research," *IEEE Access*, vol. 5, pp. 252-270, Dec. 2016.

[3] R. F. Tigrek, W. J. A. de Heij and P. van Genderen, "Multi-carrier radar waveform schemes for range and Doppler processing," *Proc IEEE 2009 Radar Conf.*, May 2009.

[4] C. Sturm, E. Pancera, T. Zwick and W. Wiesbeck, "A novel approach to OFDM radar processing," *Proc IEEE 2009 Radar Conf.*, May 2009.

[5] Y. L. Sit, C. Sturm, J. Baier and T. Zwick, "Direction of arrival estimation using the MUSIC algorithm for a MIMO OFDM radar," *2012 IEEE Radar Conf.*, May 2012.

[6] J. Li and P. Stoica, *MIMO Radar Signal Processing*. Hoboken, NJ, USA: Wiley, 2008.

[7] D. Kuswidiastuti, M. Rizky, P. H. Mukti and G. Hendrantoro, "MIMO radar waveform design using interleaved-OFDM technique," *2016 IEEE Int. Conf. Commun., Netw. Satell. (COMNETSAT)*, Dec. 2016.

[8] C. Baquero Barneto et al., "Full-Duplex OFDM Radar With LTE and 5G NR Waveforms: Challenges, Solutions, and Measurements," *IEEE Trans. Microw. Theory Tech.*, vol. 67, no. 10, pp. 4042-4054, Oct. 2019.

[9] S. D. Liyanaarachchi, et al., "Optimized Waveforms for 5G–6G Communication With Sensing: Theory, Simulations and Experiments," *IEEE Trans. Wirel. Commun.*, vol. 20, no. 12, pp. 8301-8315, Dec. 2021.

[10] R. S. Thoma et al., "Cooperative passive coherent location: A promising 5G service to support road safety," *IEEE Commun. Mag.*, vol. 57, no. 9, pp. 86–92, Sept. 2019

[11] Steffen Schieler, Christian Schneider, Carsten Andrich, Michael Döbereiner, Jian Luo, Andreas Schwind, Reiner S. Thomä, Giovanni Del Galdo, "OFDM waveform for distributed radar sensing in automotive scenarios", *Int. J. Microw. Wirel. Technol.*, vol. 12, no. 8, pp. 716-722, Oct. 2020.

[12] Prabhat Kumar Rai, Abhinav Kumar, Mohammed Zafar Ali Khan, Linga Reddy Cenkeramaddi, "LTE-based passive radars and applications: a review", *Int. J. Remote Sens.*, vol. 42, no. 19, pp. 7489-7518, Aug. 2021.

[13] L. Leyva, D. Castanheira, A. Silva, A. Gameiro and L. Hanzo, "Cooperative Multiterminal Radar and Communication: A New Paradigm for 6G Mobile Networks," *IEEE Veh. Technol. Mag.* (early access).

[14] F. Liu, C. Masouros, A. P. Petropulu, H. Griffiths and L. Hanzo, "Joint radar and communication design: applications, state-of-the-art, and the road ahead," *IEEE Trans. Commun.*, vol. 68, no. 6, pp. 3834-3862, June 2020.